

# Long time behavior of relativistic ions incessantly accelerated by an oblique shock wave

Shunsuke Usami and Yukiharu Ohsawa<sup>a)</sup>

*Department of Physics, Nagoya University, Nagoya 464-8602, Japan*

(Received 28 December 2001; accepted 29 January 2002)

Incessant acceleration of nonthermal fast ions by an oblique magnetosonic shock wave is studied with hybrid simulations. First, magnetic and electric field profiles of an oblique shock wave are obtained by means of a one-dimensional, relativistic, electromagnetic, particle simulation. Test particle trajectories of fast ions are then calculated using these wave profiles. Some fast ions are trapped by the shock wave owing to the relativistic effect that velocity is limited by the speed of light while the momentum can grow indefinitely. In these simulations, some fast ions are found to suffer energy jumps several tens of times; as a result, their final maximum Lorentz factors far exceeded 100. © 2002 American Institute of Physics. [DOI: 10.1063/1.1464147]

Particle simulations have shown that a magnetosonic shock wave can accelerate particles with several different, nonstochastic mechanisms.<sup>1–12</sup> (For theories, see Refs. 13–15.) These mechanisms can work in a shock wave with laminar structure. In a multi-ion-species plasma in which the hydrogen is the major ion component as in space plasmas, some of the hydrogen ions are accelerated via reflection by the electric potential;<sup>1–5</sup> all the heavy ions by the transverse electric field;<sup>6,7</sup> and some electrons by the electric potential and constant, cross-field electric field appearing in the wave frame.<sup>8,9</sup>

Furthermore, it was found that nonthermal, fast particles can be accelerated to higher energies by a shock wave with another mechanism.<sup>10–12</sup> A shock wave propagating perpendicular to a magnetic field  $\mathbf{B}$  can accelerate some of the fast ions with the transverse electric field.<sup>10</sup> (We assume that the shock wave propagates in the  $x$  direction with a speed  $v_{sh}$  and that  $\mathbf{B}$  points in the  $z$  direction. Thus, the transverse electric field is  $E_y$ . If  $v_{sh}$  and  $B_z$  are both positive,  $E_y$  in the laboratory frame is also positive.) Particles barely entering the shock region can go out to the upstream region again, if their velocities perpendicular to the magnetic field,  $v_{\perp}$ , are much higher than the shock propagation speed  $v_{sh}$ . While they are in the strong field region, i.e., in the shock region of strong magnetic and electric fields, they gain energy from  $E_y$  because their velocities are nearly parallel to  $E_y$ . The energy gain due to this process increases with increasing particle energy. This process could repeat a few times. However, the particles eventually move to the downstream region.

In an oblique shock wave, which is assumed to propagate in the  $x$  direction in an external magnetic field  $\mathbf{B}_0 = B_0(\cos \theta, 0, \sin \theta)$  with  $0 < \theta < \pi/2$ , this acceleration mechanism can operate several times;<sup>11</sup> if the velocity parallel to the magnetic field,  $v_{\parallel}$ , satisfies the relation  $v_{\parallel} \cos \theta \sim v_{sh}$  ( $v_{\parallel} \cos \theta$  is roughly equal to time-averaged  $v_x$  of a particle), then the particle can move with the shock wave for a long period of time. While it is in the strong field region,

perpendicular momentum  $p_{\perp}$  increases because of  $E_y$ . At the same time,  $p_{\parallel}$  rises at the moment when the particle goes in or out of the shock region.<sup>11,16,17</sup> This is due to the fact that the direction of  $\mathbf{B}$  is changed as one moves from the upstream to shock region;  $B_z$  grows while  $B_{x0}$  is constant. At the moment of the increase of  $p_{\parallel}$ , therefore, the magnitude of  $p$  is not changed and  $p_{\perp}$  is decreased. Thus, in these processes,  $p_{\parallel}$  and hence  $p_{\parallel} \cos \theta$  steadily grow. When  $v_{\parallel} \cos \theta$  exceeds the shock speed  $v_{sh}$  as a result of these effects, the particle goes away ahead of the shock wave, and the acceleration ceases.

However, it was pointed out in Ref. 11 that particles can be trapped by the shock wave, if the shock speed  $v_{sh}$  and propagation angle  $\theta$  have the relation

$$v_{sh} \sim c \cos \theta. \quad (1)$$

That is, if Eq. (1) is satisfied, particles cannot easily escape from the shock wave once they become to move with the shock wave. This is caused by the relativistic effect that, even though  $p_{\parallel}$  can increase indefinitely,  $v_{\parallel}$  is limited by the speed of light. Thus, the time-averaged velocity in the  $x$  direction ( $\sim v_{\parallel} \cos \theta$ ) cannot exceed  $c \cos \theta$ . Hence, the particle cannot go ahead of the shock wave. Under these circumstances, the acceleration process could repeat extremely many times. This mechanism could be important, for instance, around a pulsar where large-amplitude magnetosonic shock waves (or pulses) could be propagating with high propagation speeds.

In Ref. 12, an attempt was made to examine this mechanism with relativistic, electromagnetic, particle simulations. In an example in Ref. 12, a fast particle was accelerated nine times (the acceleration process continued until the end of the simulation), and its Lorentz factor increased from  $\gamma=2$  to  $\gamma=4.7$ . This simulation was terminated at  $\omega_{pe}t=5000$ , where  $\omega_{pe}$  is the spatially averaged electron plasma frequency. Because of the limitation of simulation time, very long-time behavior of particles could not be investigated.

In this Letter, we study if this mechanism works for a much longer period of time. It will be demonstrated by nu-

<sup>a)</sup>Electronic mail: ohsawa@phys.nagoya-u.ac.jp

merical simulations that owing to this relativistic trapping mechanism, some fast particles move with a shock wave for very long periods of time and suffer energy jumps several tens of times. Their Lorentz factors exceed 100.

Before showing simulation results, we analytically discuss briefly how the particle energy increases in this acceleration mechanism. If a fast particle moves with an oblique shock wave, the particle would experience one energy jump in each cyclotron period, which will be shown later in Fig. 2. The time variation of  $\gamma$  resembles a staircase.<sup>12</sup> The theory<sup>12</sup> predicts that the magnitude of one energy jump is given by

$$\delta\gamma = \frac{2q_i v_{1\perp} E_y}{m_i^2 c^2 \Omega_{i1}} \sin\left(\frac{\Omega_{i1}(t_{\text{out}} - t_{\text{in}})}{2\gamma}\right), \quad (2)$$

where  $q_i$  is the charge,  $m_i$  is the mass,  $\Omega_{i1}$  is the nonrelativistic ion cyclotron frequency,  $\Omega_{i1} = q_i B_1 / (m_i c)$ ; the subscript 1 designates quantities in the strong field region. The quantities  $t_{\text{in}}$  and  $t_{\text{out}}$  represent times when the particle goes in and out of the shock region, respectively.

The fast particles barely entering the shock region spend most of the time in the upstream region in each cyclotron period. Hence, their cyclotron periods are nearly given by  $2\pi\gamma/\Omega_{i0}$ , where  $\Omega_{i0}$  is the nonrelativistic ion cyclotron frequency in the upstream region. The cyclotron frequency  $\Omega_{i1}$  in the strong field region is related to the one in the upstream region through  $\Omega_{i1} = (B_1/B_0)\Omega_{i0}$ . By dividing Eq. (2) by  $2\pi\gamma/\Omega_{i0}$ , therefore, we obtain a differential equation for the time rate of change of  $\gamma$  of a particle accelerated many times by one shock wave as

$$\frac{d\gamma}{dt} \sim \frac{q_i v_{1\perp} E_y}{\pi m_i c^2 (B_1/B_0)} \sin\left(\frac{\Omega_{i1}(t_{\text{out}} - t_{\text{in}})}{2\gamma}\right). \quad (3)$$

This gives time dependence of  $\gamma$  averaged over the cyclotron period. For a stationary wave with a propagation speed  $v_{\text{sh}}$ , the  $z$  component of Faraday's law gives the relation  $E_y = (v_{\text{sh}}/c)(B_{z1} - B_{z0})$ . We thus have

$$\frac{d\gamma}{dt} \sim \frac{g}{\pi} \frac{v_{\text{sh}}}{c} \Omega_{i0}, \quad (4)$$

where  $g$  is a numerical factor smaller than unity,

$$g = \frac{v_{1\perp}}{c} \left(1 - \frac{B_{z0}}{B_{z1}}\right) \left(1 - \frac{B_{x0}^2}{2B_{z1}^2}\right) \sin\left(\frac{\Omega_{i1}(t_{\text{out}} - t_{\text{in}})}{2\gamma}\right). \quad (5)$$

Here, we have expanded the term  $(B_{z1}^2 + B_{x0}^2)^{-1/2}$  assuming that  $B_{z1} \gg B_{x0}$ . The quantities  $v_{1\perp}$  and  $(t_{\text{out}} - t_{\text{in}})$  may vary with time;  $(t_{\text{out}} - t_{\text{in}})$  can have different values for different cyclotron periods. If the time dependence of  $g$  averaged over  $(t_{\text{out}} - t_{\text{in}})$  is weak, roughly speaking,  $\gamma$  linearly increases with time as  $\gamma \sim (g/\pi)(v_{\text{sh}}/c)\Omega_{i0}t + \gamma_0$ , where  $\gamma_0$  is the initial value of  $\gamma$ .

Now we numerically study very long time behavior of accelerated particles. To do this, we follow test particle orbits in an oblique shock wave. For the field profiles and shock propagation speed, however, we use the ones obtained from a one-dimensional, relativistic, electromagnetic, particle simulation with full ion and electron dynamics. In so doing, we are assuming that the abundance of very fast particles is

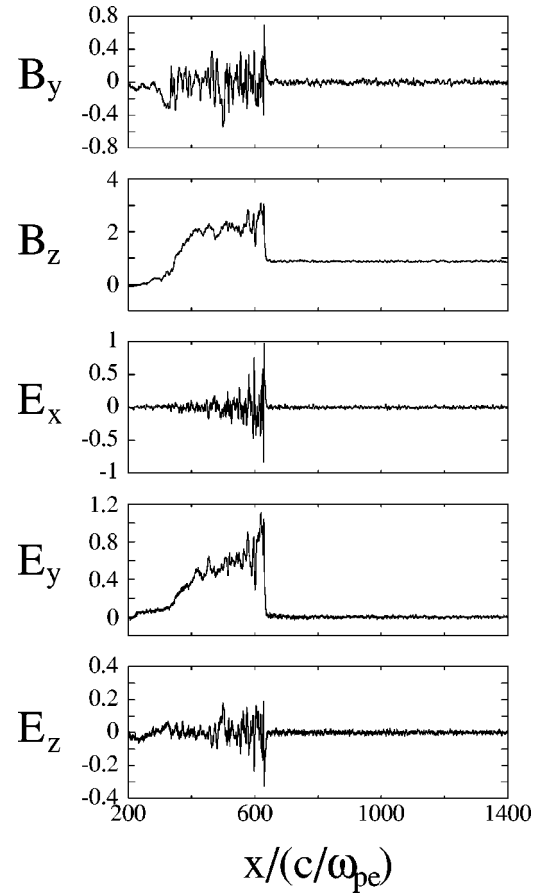


FIG. 1. Snapshots of field profiles in an oblique shock wave obtained by a particle simulation. Electric and magnetic field profiles at  $\omega_{pe}t = 1000$  ( $\Omega_{H0}t = 30$ ) are plotted. They are normalized to  $B_0$ .

much smaller than that of bulk particles; hence, we would be able to neglect the effect of fast particles on wave evolution.

We know the solitary wave solutions for small-amplitude waves.<sup>18–23</sup> However, theoretical expression for large-amplitude, collisionless shock waves has not been obtained yet. Since we need field profiles found in a self-consistent manner, we use shock waves observed in particle simulations.<sup>3,12,24</sup>

The plasma parameters in the calculations of test particle trajectories are thus the same as those in the corresponding particle simulation. The ion-to-electron mass ratio is  $m_H/m_e = 50$ ; and the electron skin depth is  $c/(\omega_{pe}\Delta_g) = 4$ , where  $\Delta_g$  is the grid spacing. The frequency ratio  $|\Omega_{e0}|/\omega_{pe}$  is 1.5 in the upstream region; for these parameters, the Alfvén speed is  $v_A/c = 0.20$ . The time step  $\Delta t$  is  $\omega_{pe}\Delta t = 0.05$ . The angle  $\theta$  ( $\tan\theta = B_{z0}/B_{x0}$ ) was taken to be  $\theta = 61^\circ$ . Numerical integration of the relativistic equation of motion was performed with Adams–Bashforth–Moulton method.<sup>25</sup>

Figure 1 shows field profiles of a shock wave with a propagation speed  $v_{\text{sh}} = 2.4v_A$ , which is very close to  $c \cos 61^\circ$ . The grid size of this particle simulation was 8192. The number of simulation particles was  $N_e = 576\,000$  for electrons; as space plasmas, the code included helium as well as hydrogen with their mass density ratio  $n_{\text{He}}m_{\text{He}}/(n_{\text{H}}m_{\text{H}}) = 0.4$ . Then, we followed test particle trajectories in this

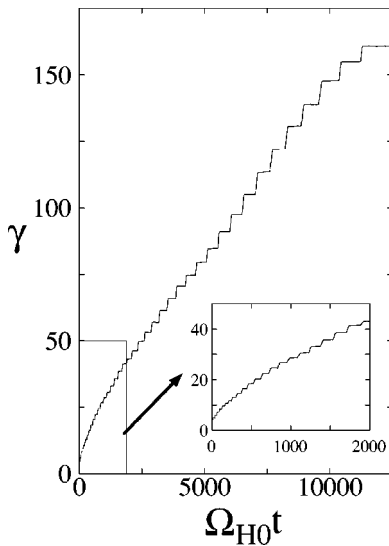


FIG. 2. Time variation of  $\gamma$  of a repeatedly accelerated fast ion.

shock wave assuming it continues to propagate with stationary field profiles; the profiles at  $\Omega_{H0}t = 30$  were used. Figure 2 shows the time variation of Lorentz factor  $\gamma$  of an accelerated test particle. An expanded view of the early stage is also presented in the small panel. We observe that  $\gamma$  increased stepwise 42 times from  $\gamma = 4.2$  to  $\gamma \approx 160$ . At  $\Omega_{H0}t = 1.1 \times 10^4$ , the particle escaped from the shock wave to the upstream region. The time intervals and magnitudes of energy jumps both grow with time. This is because the gyroperiod and gyroradius become longer as  $\gamma$  goes up. Consequently, gyroaveraged  $\gamma$  rises almost linearly with time, as suggested earlier.

Figure 3 displays time variations of other physical quantities. The top panel shows the  $x$  position of the particle relative to the shock wave,  $X = (x - v_{sh}t) / (c / \omega_{pe})$ . Here,  $X = 0$  represents the position of the shock front. Accordingly,  $X$  is negative when the particle is in the shock region. For  $\Omega_{H0}t < 1.1 \times 10^4$ , the minima of  $X$  are negative, indicating that this particle moved with the shock wave for a very long period of time. The parallel momentum  $p_{\parallel}$  grows steadily, while  $p_{\perp}$  rapidly changes when it is in the shock region. It is interesting to note that the increase in  $p_{\parallel}$  occurs when the particle goes out of the shock wave whereas  $p_{\parallel}$  slightly decreases when the particle goes in the shock wave. This difference will be discussed in detail elsewhere. We also note that  $v_{\parallel}$  is limited by  $c$ . The average value of  $v_{\perp}$ , i.e.,  $v_{\perp}$  in the shock region, is  $v_{\perp} / c = 0.2 \sim 0.3$ . The velocity  $v_x$  oscillates around the shock speed  $v_{sh}$ , which is indicated by the dashed line. From the observed average values of  $v_{\perp} / c$ ,  $B_{z0} / B_{z1} (= 0.3 \sim 0.5)$ , and  $\sin[\Omega_{i1}(t_{out} - t_{in})] / (2\gamma)$  ( $\sim 0.7$ ), we find from Eq. (5) that  $g = 0.07 \sim 0.13$ . On the other hand, from the average slope of  $\gamma$  in Fig. 2 for  $1.4 \times 10^3 < \Omega_{H0}t < 1.1 \times 10^4$ , we can estimate  $g$  in this case as  $\sim 0.09$ , using Eq. (4).

We show in Fig. 4 another curious example. Here, the increase in  $\gamma$  stops at  $\Omega_{H0}t = 4.1 \times 10^3$ . After a short while, however,  $\gamma$  begins to rise again at  $\Omega_{H0}t = 5.3 \times 10^3$ . That is, the particle once escaped from the shock wave to the up-

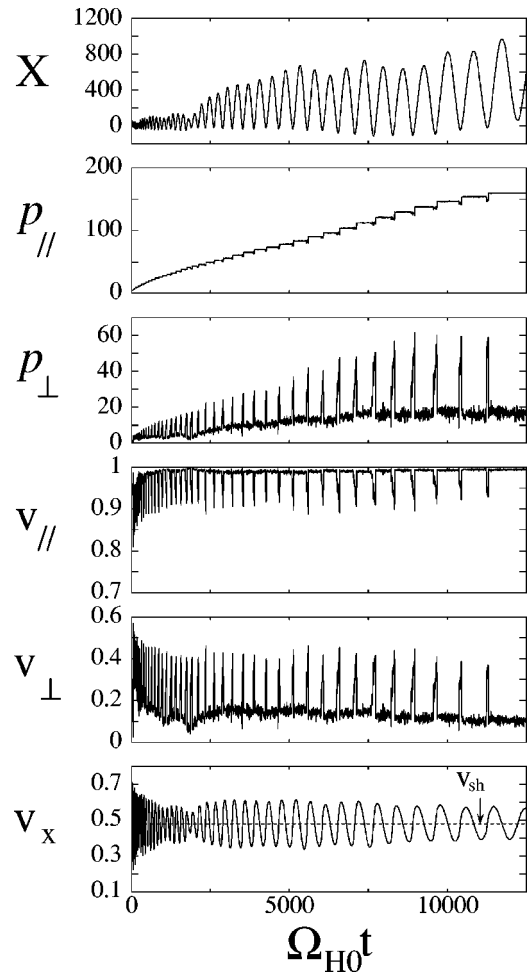


FIG. 3. Time variations of the particle position, momentum, and velocity. Here, the momentum and velocity are normalized to  $m_Hc$  and  $c$ , respectively.

stream region. However, because of the small fluctuation of the fields that happen to be in front of the shock wave,  $v_{\parallel}$  of the particle was slightly reduced. (Since the field profiles were taken from the particle simulation, they include various

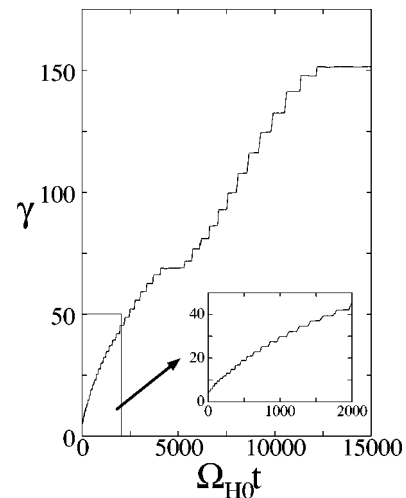


FIG. 4. Time variation of  $\gamma$ . This particle is trapped again after once de-trapped.

fluctuations.) The particle was therefore overtaken by the shock wave. The acceleration thus began again. This might be a rather rare example. It indicates, however, that the trapping of particles is quite stable.

In summary, we have studied the incessant acceleration of fast ions by means of hybrid simulations. Electromagnetic field profiles of an oblique shock wave were obtained with a one-dimensional, relativistic, electromagnetic, particle simulation with full ion and electron dynamics. Test particle trajectories in the shock wave are then calculated. It has been found that some fast ions are trapped for extremely long periods of time by the shock wave. This is due to the relativistic effect that the particle speed is limited by the speed of light while the momentum can increase indefinitely. These particles experience energy jumps many times. In the simulations, their final Lorentz factors far exceeded 100.

<sup>1</sup>D. Biskamp and H. Welter, Nucl. Fusion **12**, 663 (1972).

<sup>2</sup>D. W. Forslund, K. B. Quest, J. U. Brackbill, and K. Lee, J. Geophys. Res., [Oceans] **89**, 2142 (1984).

<sup>3</sup>Y. Ohsawa, Phys. Fluids **28**, 2130 (1985).

<sup>4</sup>B. Lembège and J. M. Dawson, Phys. Fluids B **1**, 1001 (1989).

<sup>5</sup>R. L. Tokar, S. P. Gary, and K. B. Quest, Phys. Fluids **30**, 2569 (1987).

<sup>6</sup>M. Toida and Y. Ohsawa, J. Phys. Soc. Jpn. **64**, 2036 (1995).

<sup>7</sup>M. Toida and Y. Ohsawa, Sol. Phys. **171**, 161 (1997).

<sup>8</sup>N. Bessho and Y. Ohsawa, Phys. Plasmas **6**, 3076 (1999).

<sup>9</sup>N. Bessho and Y. Ohsawa, Phys. Plasmas **7**, 4004 (2000).

<sup>10</sup>K. Maruyama, N. Bessho, and Y. Ohsawa, Phys. Plasmas **5**, 3257 (1998).

<sup>11</sup>T. Masaki, H. Hasegawa, and Y. Ohsawa, Phys. Plasmas **7**, 529 (2000).

<sup>12</sup>S. Usami, H. Hasegawa, and Y. Ohsawa, Phys. Plasmas **8**, 2666 (2001).

<sup>13</sup>R. Z. Sagdeev and V. D. Shapiro, Zh. Eksp. Teor. Fiz. Pis'ma Red. **17**, 387 (1973) [JETP Lett. **17**, 279 (1973)].

<sup>14</sup>Y. Ohsawa, J. Phys. Soc. Jpn. **59**, 2782 (1990).

<sup>15</sup>M. A. Lee, V. D. Shapiro, and R. Z. Sagdeev, J. Geophys. Res., [Oceans] **101**, 4777 (1996).

<sup>16</sup>T. P. Armstrong, G. Chen, E. T. Sarris, and S. M. Krimigis, in *Study of Traveling Interplanetary Phenomena*, edited by M. A. Shea and D. F. Smart (Reidel, Dordrecht, 1977), p. 367.

<sup>17</sup>R. B. Decker, Space Sci. Rev. **48**, 195 (1988).

<sup>18</sup>C. S. Gardner and G. K. Morikawa, Commun. Pure Appl. Math. **18**, 35 (1965).

<sup>19</sup>T. Kakutani, H. Ono, T. Taniuti, and C. C. Wei, J. Phys. Soc. Jpn. **24**, 1159 (1968).

<sup>20</sup>Y. Ohsawa, Phys. Fluids **29**, 1844 (1986).

<sup>21</sup>J. H. Adlam and J. E. Allen, Philos. Mag., Suppl. **3**, 448 (1958).

<sup>22</sup>L. Davis, R. Lüst, and A. Schlüter, Z. Naturforsch. A **13**, 916 (1958).

<sup>23</sup>Y. Ohsawa, Phys. Fluids **29**, 2474 (1986).

<sup>24</sup>P. C. Liewer, A. T. Lin, J. M. Dawson, and M. Z. Caponi, Phys. Fluids **24**, 1364 (1981).

<sup>25</sup>W. H. Press, S. A. Teukolsky, W. T. Vetterling, and B. P. Flannery, *Numerical Recipes in Fortran* (Cambridge University Press, New York, 1992), Chap. 16.